

## Electrical conductivity measurements of strongly coupled W plasmas

S. Saleem,\* J. Haun, and H.-J. Kunze

*Institut für Experimentalphysik V, Ruhr-Universität, 44780 Bochum, Germany*

(Received 23 April 2001; published 15 October 2001)

Nonideal plasmas of tungsten were produced by vaporizing thin wires of 0.1 mm and 0.3 mm in diameter in small glass capillaries (in air) by means of a short-pulse current from an electrical discharge. For a short period of time, the inner wall of the rigid glass capillary confines the plasma until the induced pressure shock wave disintegrates the capillary. Spectroscopic measurements were carried out on the ejected plasma close to the end of the capillary. The plasma temperature was obtained by fitting a Planck function to the measured continuum spectrum. The resistance was derived from the voltage across the plasma and the current through the plasma. The plasma radius was determined with an intensified charge-coupled device camera and a streak camera and allowed the derivation of the conductivity. Particle densities were of the order of  $10^{22}$  particle/cm<sup>3</sup> and electron temperatures were in the range from 10 kK to 22 kK. These measurements are compared with theoretical models and previous work.

DOI: 10.1103/PhysRevE.64.056403

PACS number(s): 52.25.Fi, 52.25.Jm, 52.25.Os, 72.15.-v

### I. INTRODUCTION

The electrical conductivity  $\sigma$  is a fundamental quantity of plasmas and not well known for high-density and low-temperature plasmas, i.e., for so-called strongly coupled or nonideal plasmas. It determines the dissipative heating of the plasma and its interaction with an external field. The electrical conductivity is very sensitive to the electron states. During the transition from a metal through the liquid phase to a weakly conducting gas phase it varies from a state of almost free electrons to electrons strongly bound to atoms and hence a phase of low conductivity. Then by ionization the electrical conductivity increases again by several orders of magnitude. Tungsten has a wide range of applications in industry and in other fields; tungsten wires are used, e.g., in x-ray tubes, electron microscopes, and electron microprobes, taking advantage of the high temperature for melting (3680 K) and evaporation. The conductivity of the corresponding plasmas is of great interest, therefore, and we applied the recently developed technique [1,2] of rapidly vaporizing and heating a thin wire in a glass capillary by the current from a suitable discharge to generate these plasmas for such studies. The glass capillary provides confinement of the plasma for some time, and thus a reasonably well defined density. In [3] the method was modified and water was employed as confining medium. After discharging a capacitor through the thin wire, sufficient energy has been supplied to the wire to change it into a plasma. Resistance and plasma temperature are measured as function of time using optical and electrical methods as we will see later. Previous studies in our laboratory focused on the conductivity of plasmas of copper [1], aluminum [2], zinc [4], and carbon [5]. Now we turn to tungsten as an example of a metal with a high melting temperature. The results will be compared with other experiments and with theoretical calculations. High-density low-temperature plasmas are usually strongly coupled and are characterized by the Coulomb coupling parameter  $\Gamma$  for the ions and the de-

generacy parameter  $\theta$  for the electrons, in addition to the plasma temperature, mass density, and electron density [6].  $\Gamma$  is a measure of the Coulomb interaction and is defined as the ratio of average Coulomb interaction energy to average kinetic energy:

$$\Gamma = \frac{Z^2 e^2}{4\pi\epsilon_0 a k_B T} = 2.69 \times 10^{-5} \frac{Z^2 \sqrt[3]{n_i}}{T}, \quad (1)$$

where  $a = (3/4\pi n_i)^{1/3}$  is the ion-sphere radius,  $Z$  is the average ionization state,  $n_i$  is the ion density in m<sup>-3</sup>, and  $T$  is the plasma temperature in K. The degeneracy parameter used as a measure of the level of degeneracy of the electrons is

$$\theta = \frac{k_B T}{E_F} = \frac{2m_e k_B T}{\hbar^2 (3\pi^2 n_e)^{2/3}} = 2.36 \times 10^{14} \frac{T}{\sqrt[3]{n_e}}, \quad (2)$$

where  $E_F$  denotes the Fermi energy,  $n_e$  the electron density in m<sup>-3</sup>, and  $m_e$  the mass of the electron. The dependence of the electrical conductivity  $\sigma$  on the coupling parameter and temperature will be discussed and analyzed in the last section. For the plasmas studied in this investigation typically  $\Gamma \geq 1$ , i.e., the plasmas are strongly coupled with the electrons being slightly degenerate,  $\theta \leq 1$ .

### II. DESCRIPTION OF EXPERIMENTAL SETUP AND EXPERIMENT

A schematic diagram of the apparatus is shown in Fig. 1. The capillary tube 6 mm in diameter (arrow 1) has a bore of 0.8 mm and a length of 24 mm. With the tungsten wire inside it is placed between brass electrodes (arrow 4), and the ends are lightly clamped to contact the ends of the wire. The tungsten wire (arrow 2) has a purity of approximately 99.98%, a length 24 mm, and wires of diameters 0.3 mm and 0.1 mm were used. A capacitor bank of 3.86  $\mu$ F charged to 10–24 kV as a source of energy is connected with the electrodes (arrow 4) and is discharged through the tungsten wire. The brass electrodes are isolated by a thick plastic cover (arrow 3). For the observation of the time history of the

\*Permanent address: Zagazig University, Egypt.

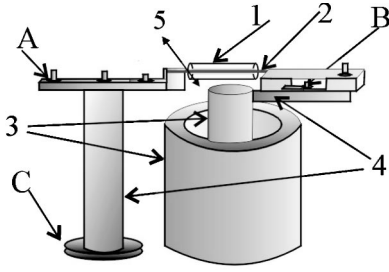


FIG. 1. Schematic of the apparatus. *A* and *B* are connections to the voltage dividers, *C* is the Rogowski coil, 1 is the capillary, 2 is the wire, 3 is an insulator, 4 are the electrodes, and 5 indicates the directions of observation.

diameter of the plasma column the visible light emitted from the plasma (arrow 5) is focused onto a slit oriented perpendicular to the wire, and this slit is imaged again onto the cathode of a streak camera sweeping the image at 50 ns/mm in the plane of the film. Three types of film were used with the streak camera: Polaroid 667 for calibration, and Kodak Tmax 400 and Ilford HP5 for measuring the plasma radius as a function of time. The pulse from a ruby laser was used as time reference, and it is seen as a vertical line at the left side of the streak photographs. For checking the homogeneity of the whole plasma column the streak camera could be replaced by an intensified charge-coupled device (ICCD) camera and photos of the full plasma column could be taken. Light emitted into the direction opposite to the camera was split into two beams by a glass plate in the optical path; one beam was focused onto a 1/8 m monochromator equipped with an optical multichannel analyzer for recording the full spectrum from about 380 nm to 700 nm. The relative sensitivity of the system was determined using a tungsten ribbon lamp. The other beam was focused onto a 1/4 m monochromator with a photomultiplier to record the time evolution of the emission at 655 nm. The discharge current waveform, monitored by a Rogowski coil (arrow *C*), was typical of that of overdamped *LCR* circuits. The rate of rise of the current being limited by the total circuit inductance (154 nH), the load wire inductance was typically about 30 nH for wires 0.3 mm in diameter and 29.4 nH for wires 0.1 mm in diameter. The voltage *V* across the wire/plasma is measured by two voltage dividers, each connected to one of the electrodes. The voltage consists of an inductive component  $LdI/dt + IdL/dt$  and the resistive component  $IR$  of interest. At the beginning of the discharge when resistance and current are very low, the inductive term even dominates. At later times, when the plasma fills the capillary,  $IdL/dt$  is negligible. The resistance *R* of the confined plasma is thus simply obtained from

$$R = \frac{V - LdI/dt}{I}, \quad (3)$$

leading to the conductivity  $\sigma$  via

$$\sigma = \frac{l}{\pi r_p^2(t)R(t)}, \quad (4)$$

*l* being the length of the plasma (capillary) and  $r_p$  its radius. As recognized already in Ref. [7] the effects of the magnetic field on the resistance are negligible because the electron collision frequency is much higher than the electron cyclotron frequency. The plasma is thus isotropic and the conductivity a scalar quantity. The exploding tungsten wire in the glass capillary can be described approximately as follows. Initially the very high current pulse,  $I_{\max} \sim 36$  kA, which depends on the cross section of the tungsten wire, heats the wire up to its melting point and then to temperatures higher than the boiling point of the metal. This part of the explosion lasts typically several hundred nanoseconds depending on the *LCR* circuit parameters. At this time the electron mean free path is very short in the high-density metal gas and the resistance of the vaporized wire increases sharply and the current decreases by several orders of magnitude. Virtually no light is emitted during this early period as the high-pressure gas expands; the pressure then decreases and impact ionization can occur as the electron mean free path increases. The current rise time was usually about  $\sim 710$  ns at 16 kV charging voltage for wires 0.3 mm in diameter, the circuit frequency being  $f \sim 170$  kHz. For homogeneous heating of the wires it is crucial that the current density is nearly constant over the cross section of the wires. This is indeed the case as estimates of the skin depth show. For a conductor with conductivity  $\sigma$  and permeability  $\mu$ , the skin depth  $\delta$  is given by

$$\delta = \frac{1}{\sqrt{\pi f \sigma \mu}}. \quad (5)$$

For all wires employed the skin depth was larger than the diameter of the wires ( $\delta = 0.28$  mm). At our relatively slow rates of energy input we also should check if radiation losses could inhibit vaporization of the wire. The radiation losses of a blackbody of surface *A* are given by

$$\left(\frac{dE}{dt}\right)_{\text{rad}} = \sigma_0 A (T^4 - T_0^4), \quad (6)$$

where  $\sigma_0 = 5.67 \times 10^{-8} \text{ W/m}^2 \text{ K}^4$  is the Stefan-Boltzmann constant, and  $T_0$  and *T* are the ambient temperature and the temperature of the blackbody, respectively. At the boiling point of tungsten ( $T = 5800$  °K) the losses of a wire 0.3 mm in diameter and 24 mm in length are thus 1.45 kW, and of a wire 0.1 mm in diameter at the same length 0.48 kW. This is small compared with the input power ( $> 4 \times 10^5$  kW) and hence only a very small fraction is not available for heating, melting, and vaporization. Measurements of the resistance are meaningful only after the wires are completely vaporized. Assuming a thermodynamically reversible vaporization process [8], the total energy needed for that may be calculated. For the wire 0.3 mm in diameter (mass 32.75 mg) this energy is 170 J and has been input at a time 975 ns after beginning of the discharge; for the wire 0.1 mm in diameter the necessary input has already been completed after 485 ns [see later in Fig. 3(c)].

### III. THEORY

In the low-density limit the conductivity  $\sigma$  of ideal plasmas is usually described by the standard Spitzer theory [9]

$$\sigma_{Sp} = \gamma_E 2.63 \times 10^{-4} \frac{T^{3/2}}{Z \ln \Lambda} \frac{1}{\Omega \text{ cm}}, \quad (7)$$

where  $\ln \Lambda$  is the Coulomb logarithm and the factor  $\gamma_E$  depends on the average degree of ionization  $Z$ ; for  $Z=1$ , for example,  $\gamma_E=0.582$ . For nonideal plasmas the usual definition of the Coulomb logarithm is slightly modified [10]. In the opposite limit the Ziman theory gives the conductivity for liquid metals [11]. It is based on a functional relation similar to the Drude theory,

$$\sigma_e = \frac{n_e e^2}{m v_F} \Lambda_e, \quad (8)$$

which merely includes scattering of the free electrons at the thermal oscillations of the metal grid.  $\Lambda_e$  is the mean free path length of the electrons and  $v_F$  is the Fermi velocity, which depends on the electron density. The calculation of  $\Lambda_e$  usually requires knowing the ion structure factor. For temperatures above the melting temperature  $T_m$ , it is approximated by

$$\Lambda_e = 50a \frac{T_m}{T} \frac{1}{\gamma}, \quad (9)$$

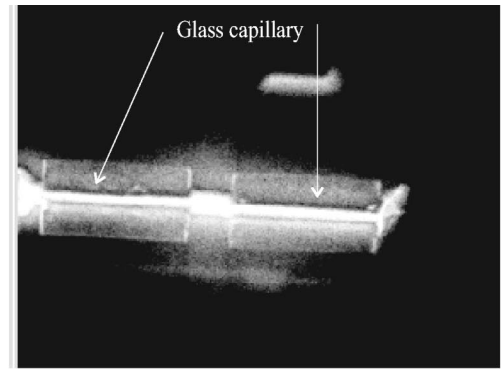
where  $a$  is the interatomic distance and the constant  $\gamma$  is chosen for each metal to correctly give the increase in resistivity at melting. The melting temperature itself may be calculated according to [10]

$$T_m = 0.32 \left[ \frac{\xi}{1 + \xi} \right]^4 \xi^{2b-2/3} \text{ eV}, \quad (10)$$

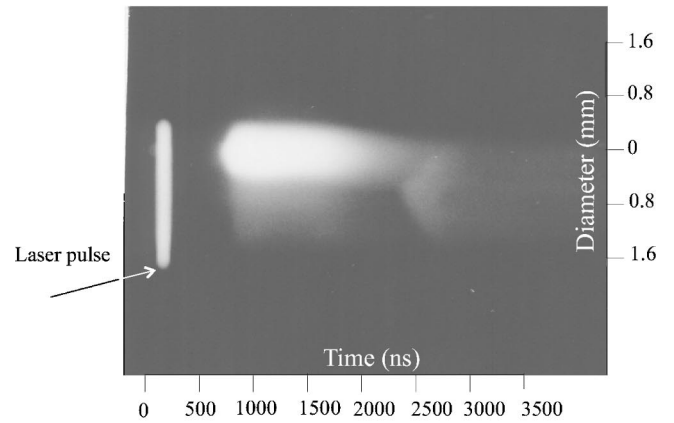
where  $b=0.6Z^{1/9}$ ,  $\xi=9.0Z^{0.3}\rho/A$ ,  $Z$  is the nuclear charge,  $\rho$  the mass density, and  $A$  the atomic weight. For the regime of nonideal plasmas between the above limits, various methods have been applied to modify appropriately the standard Spitzer theory on the one end and to extend the Ziman theory on the other end. They are referred to in Ref. [12]; these authors calculated the conductivity within the linear response theory, which also reproduces in the appropriate limits both the Spitzer and Ziman theories.

### IV. RESULTS AND DISCUSSION

The voltage and current and hence the resistance are measured during the whole discharge, but the interpretation of the resistance in terms of a conductivity is meaningful only at times when the plasma is homogeneous along the axis. The homogeneity therefore was checked by photographs. Figure 2(a) shows such a photograph taken at 1165 ns after the beginning of the discharge in a case where the capillary was split for observation in the midplane. Figure 2(b) gives an example of a streak photograph of the expanding wire/plasma, which allows the determination of the radius of the



(a)



(b)

FIG. 2. (a) Photograph of glass capillary and tungsten plasma taken with an ICCD camera (gate time 40 ns) at 1165 ns after the beginning of the discharge. The diameter of the tungsten wire was 0.3 mm; the initial voltage at the capacitor was 16 kV. (b) Streak photograph of an exploding tungsten wire 0.3 mm in diameter, 16 kV initial capacitor voltage.

plasma and of the time when the plasma hits the inner wall. This enables the derivation of the plasma density from the original mass of the wire assuming that the losses through the ends of the capillary are small. The use of two wires of different diameters resulted in different densities, and driving the discharge through the wires at different voltages and hence with different currents led to different temperatures of the plasmas due to different Ohmic heating.

Figure 3(a) shows current through and voltage across the wire for three different charging voltages of the capacitor. As discussed in Sec. II, vaporization is completed after about 1000 ns and the plasma hits the wall at around 1100 ns. For the 0.1 mm diameter wire these times are 500 ns and 600 ns, respectively. Figures 3(b) and 3(c) give the resistance of the wire/plasma according to Eq. (3) and the power input into the wire as well as the accumulated energy deposited in the wire. Figure 4 displays the mass density calculated from the observed radius of the plasma and the temperature for the case of 16 kV charging voltage on the capacitor. It was derived by fitting a Planck function to the spectrum emitted in the wavelength range from about 420 nm to 550 nm. It is not

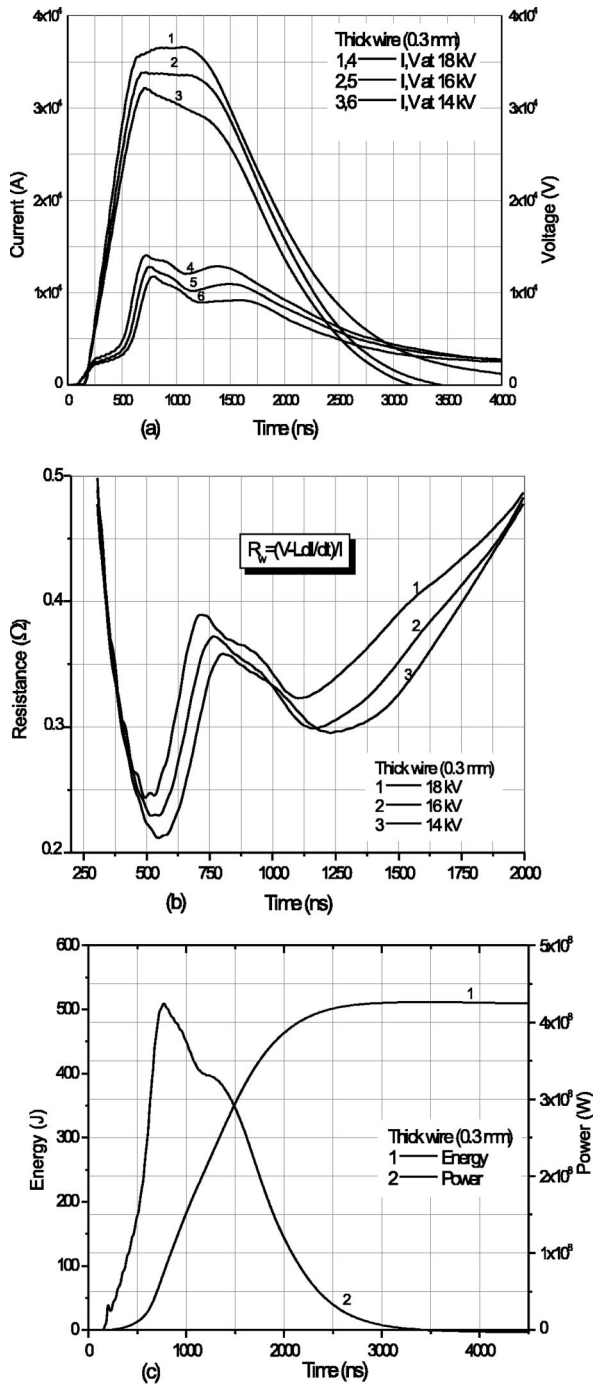


FIG. 3. (a) Current through and voltage across the wire as functions of time for the discharge through a tungsten wire 0.3 mm in diameter, for three different charging voltages of the capacitor. (b) Resistance of wire/plasma. (c) Power into the wire and accumulated energy deposited in the wire.

possible to infer the charge composition from our observations. In general, it will be multispecies. For tungsten it was calculated by Kuhlbrodt and Redmer [12] using a system of coupled mass action laws with corrections for pressure ionization. For our range of densities and temperatures they obtain an average charge  $Z \approx 0.7$ , revealing that the plasmas are partially ionized.

The conductivities derived from the measurements with

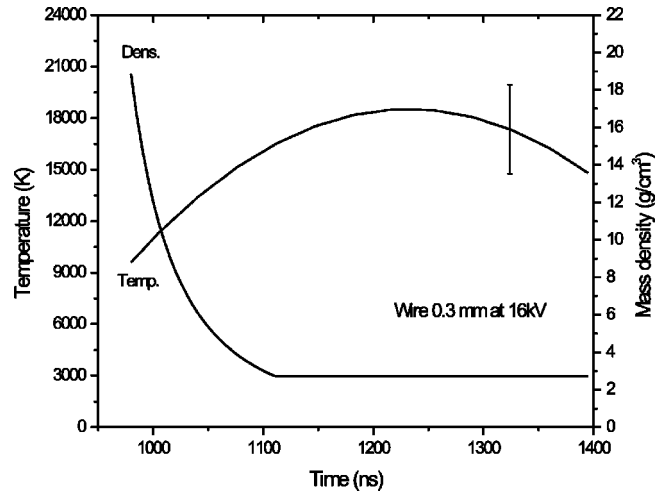


FIG. 4. Density and temperature as functions of time for the 0.3 mm diameter wire. The typical error is 15% for the temperature and it is indicated for one time.

the thick and the thin wires are finally shown as functions of the mass density in Fig. 5. The error is estimated to be about 15%. The temperature is different for different mass densities, and therefore an average temperature is indicated for three density ranges. For comparison experimental values obtained by DeSilva and Katsouros [13] are given; they employed wires confined by water. At higher mass densities and low temperatures, where according to Kloss *et al.* [14] the conductivity is weakly dependent on the temperature, the agreement between the two measurements is very good. At lower densities some deviations occur due to the different energy input used resulting in different temperatures. At the higher densities tungsten is still liquid and conductivities obtained by Seydel *et al.* [15] and by Kloss *et al.* [14] for the temperature range from 4 kK to 13 kK are also plotted. Because of the negligible temperature dependence in this range it is meaningful to compare these conductivities with theo-

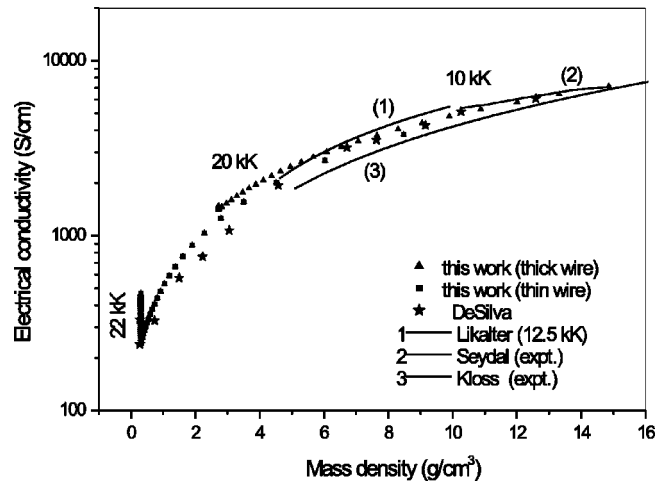


FIG. 5. Experimental conductivity. For comparison experimental results of DeSilva *et al.* [13], Seydel *et al.* [15], as well as of Kloss *et al.* [14] are given in addition to theoretical calculations by Likalter [16] for the high-density range.

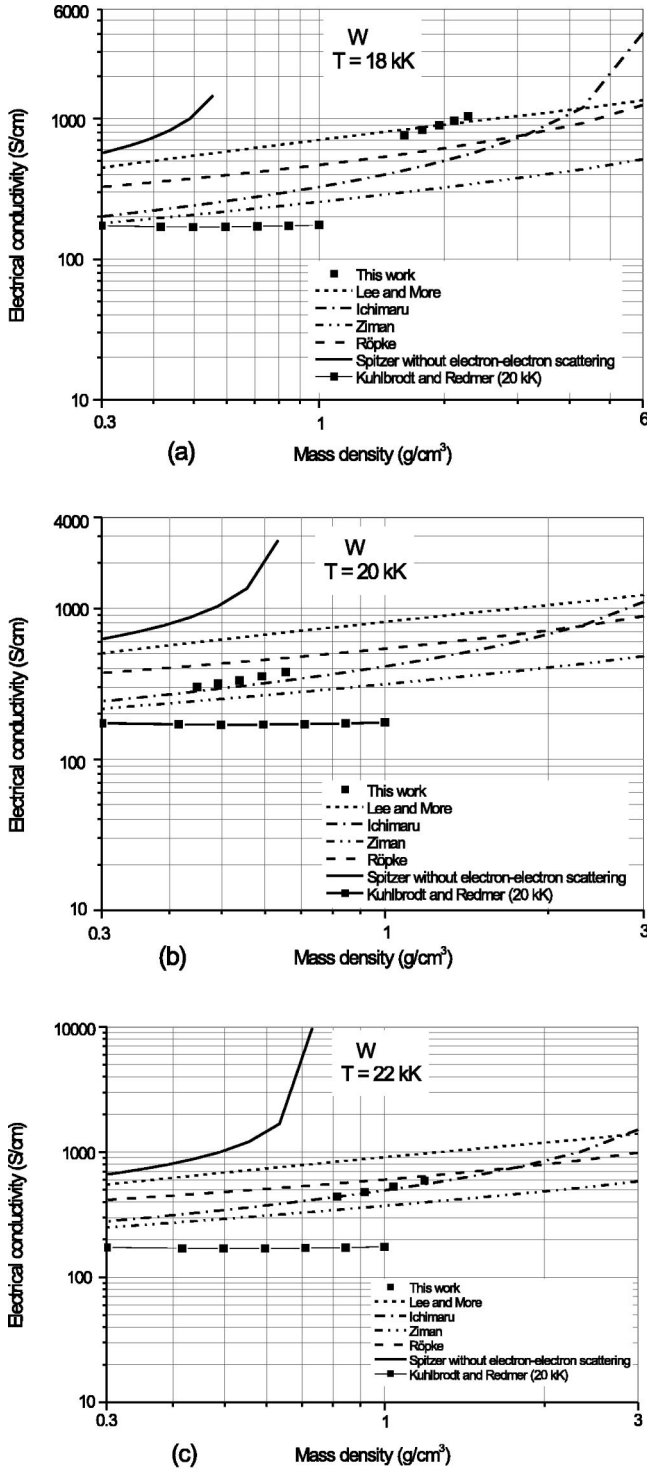


FIG. 6. Comparison of the experimental conductivities with various theoretical calculations.

retical calculations by Likalter for one temperature (12.5 kK) [16], which just corresponds to the critical temperature (curve 1 of Fig. 5). The agreement is indeed satisfactory.

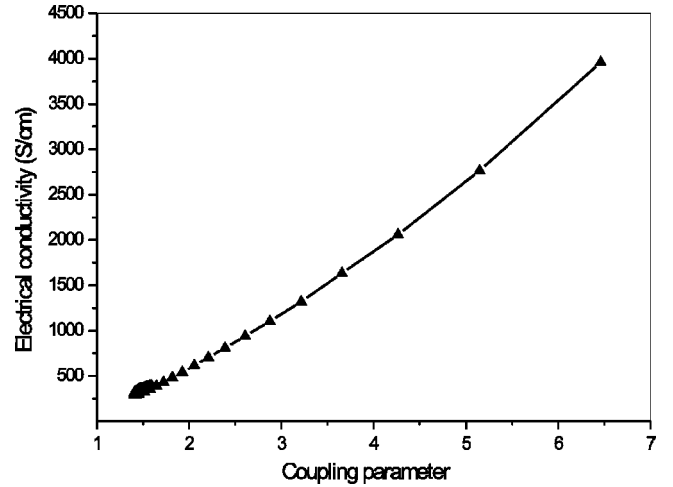


FIG. 7. Conductivity as a function of the coupling parameter.

Our conductivities in the lower-density range are compared with several theoretical calculations for three temperatures in Fig. 6. They are calculations by Lee and Moore [10], by Ichimaru [6], by Ziman [11], by Kuhlbrodt and Redmer [12], and by Röpke [17], and results obtained according to the Spitzer theory [9]. At mass densities of  $1 \text{ g/cm}^3$  and below the best agreement is with the Ziman theory.

It is interesting to plot the conductivity as a function of the coupling parameter. This is illustrated for low mass densities in Fig. 7. We find that  $\sigma$  is quite well approximated by

$$\sigma = 180\Gamma^{5/3} \text{ S/cm} \quad (11)$$

with no additional dependence on temperature. This holds for the range  $1 \leq \Gamma \leq 7$ . The comparison with the results obtained for Cu plasmas [1] indicates that the scaling with  $\Gamma^{5/3}$  also holds quite well in the above range although the absolute values are different.

## V. CONCLUSIONS

We have measured electrical conductivity and plasma temperature for rapidly vaporized tungsten wires confined in glass capillaries and compared the results with theoretical calculations. Temperatures were in the range from 10 to 22 kK; mass densities were between 0.4 and  $15 \text{ g/cm}^3$ . For coupling parameters between 1 and 7 a rather simple dependence solely on the coupling parameter is found.

## ACKNOWLEDGMENTS

One of us (S.S.) acknowledges support from the Ministry of Higher Education of the Arab Republic of Egypt and thanks colleagues Zeljko Andreic (Zagreb), Ivonne Möller, Markus Kaczor, Thomas Wrubel, and Stefan Seidel for helpful suggestions and encouragement. We thank A. W. DeSilva (College Park), S. Kuhlbrodt (Rostock), and R. Redmer (Rostock) for sending us their experimental and theoretical data.

- [1] A.W. DeSilva and H.-J. Kunze, Phys. Rev. E **49**, 4448 (1994).
- [2] I. Krisch and H.-J. Kunze, Phys. Rev. E **58**, 6557 (1998).
- [3] A.W. DeSilva and J.D. Katsouros, Phys. Rev. E **57**, 5945 (1998).
- [4] J. Haun, Contrib. Plasma Phys. **40**, 126 (2000).
- [5] J. Haun and H.-J. Kunze, Contrib. Plasma Phys. **39**, 169 (1999).
- [6] S. Ichimaru, Rev. Mod. Phys. **54**, 1015 (1982).
- [7] R.L. Shepherd, D.R. Kania, and L.A. Jones, Phys. Rev. Lett. **61**, 1278 (1988).
- [8] P. Thomas and R.D. Sacks, Anal. Chem. **50**, 1084 (1978).
- [9] L. Spitzer, *Physics of Fully Ionized Gases* (Wiley, New York, 1962).
- [10] Y.T. Lee and R.M. Moore, Phys. Fluids **27**, 1273 (1984).
- [11] J. M. Ziman, *Principles of the Theory of Solids* (Cambridge University Press, London, 1972).
- [12] S. Kuhlbrodt and R. Redmer, Phys. Rev. E **62**, 7191 (2000).
- [13] A. W. DeSilva and J. D. Katsouros (private communication).
- [14] A. Kloss, H. Hess, and H. Schneidenbach, High Temp.-High Press. **29**, 215 (1997); A. Kloss, T. Motzke, R. Grossjohann, and H. Hess, Phys. Rev. E **54**, 5851 (1996).
- [15] U. Seydel, W. Fücke, and H. Walde, *Die Bestimmung thermo-physikalischer Daten Flüssiger Hochschmelzender Metalle mit Schnellen Pulsaufheizexperimenten* (Verlag Dr. Peter Mannkopf, Düsseldorf, 1980), p. 156.
- [16] A.A. Likalter, Sov. Phys. Usp. **35**, 591 (1992); Phys. Scr. **55**, 114 (1997).
- [17] G. Röpke, Phys. Rev. A **38**, 3001 (1988).